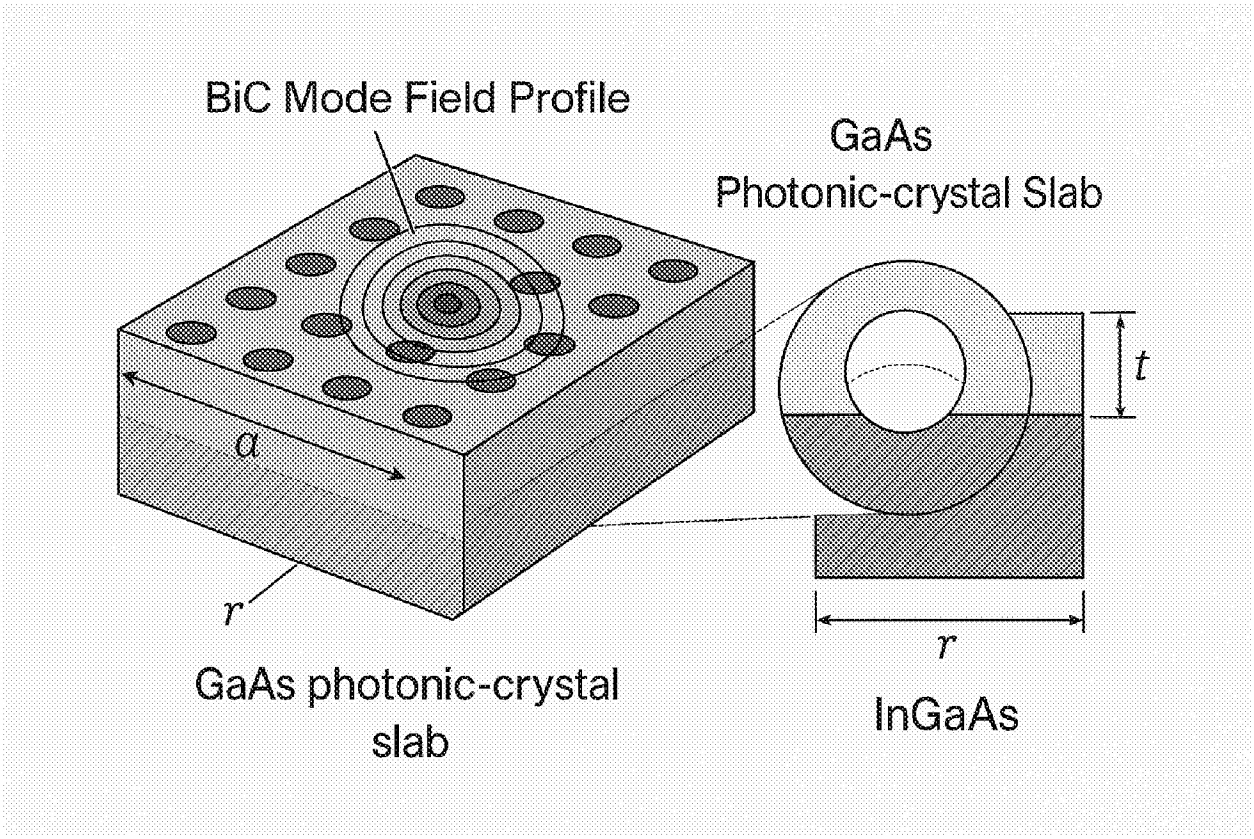

Figure 1. Perspective and cross-section of the GaAs/InGaAs photonic-crystal slab (period a, hole radius r, slab thickness t) with the bound-state-in-continuum (BiC) mode field profile sketched in blue concentric contours.

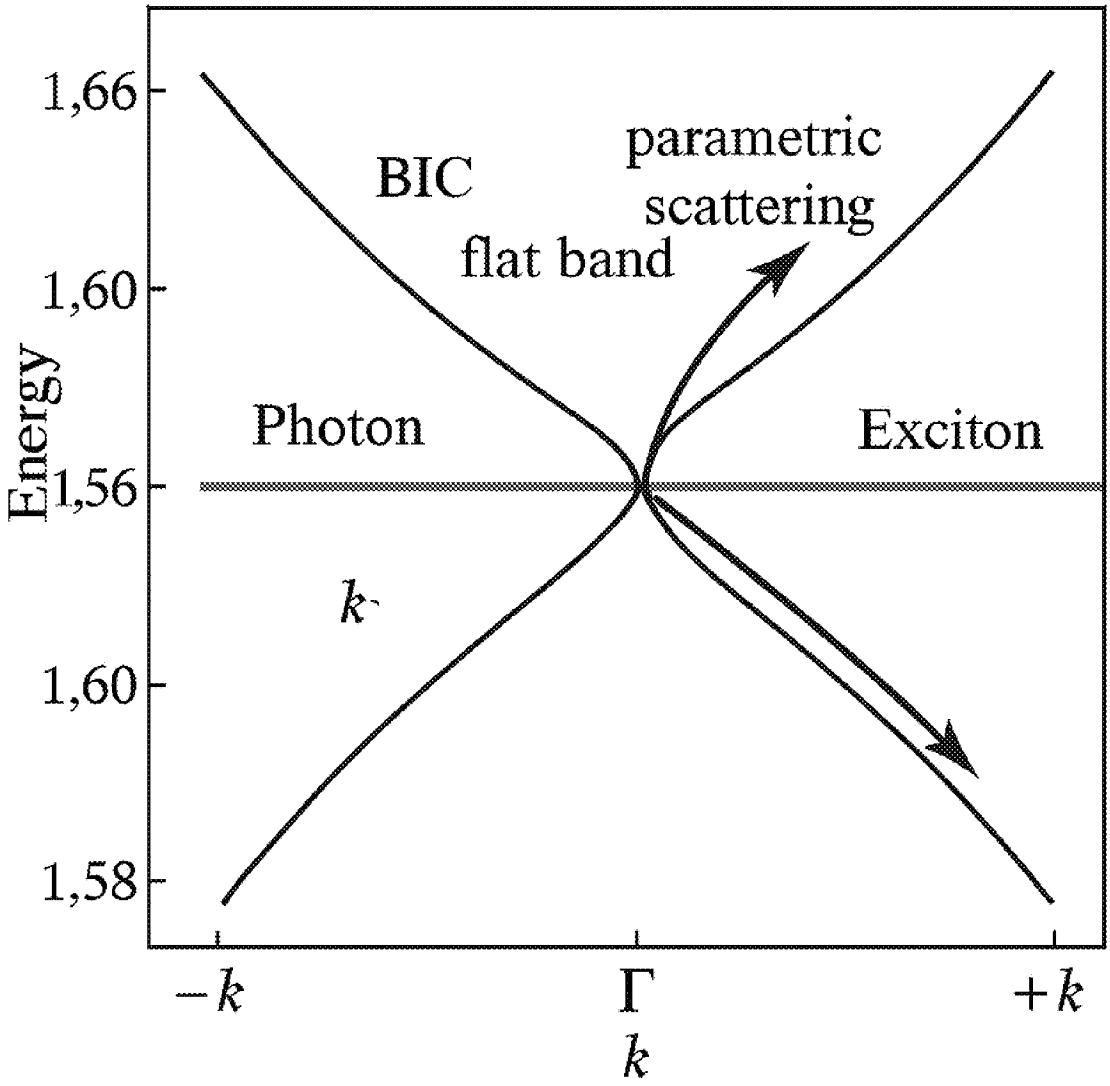

Figure 2. Calculated polariton dispersion at the Γ-point: the symmetry-protected BiC appears as an almost flat blue band crossing the exciton resonance (horizontal), while the photon-like branches (black) curve upward and downward. Arrows mark parametric scattering from the $k \approx 0$ condensate into $\pm k$ side-modes that lock to form the supersolid lattice period $\Lambda = \pi/k$.

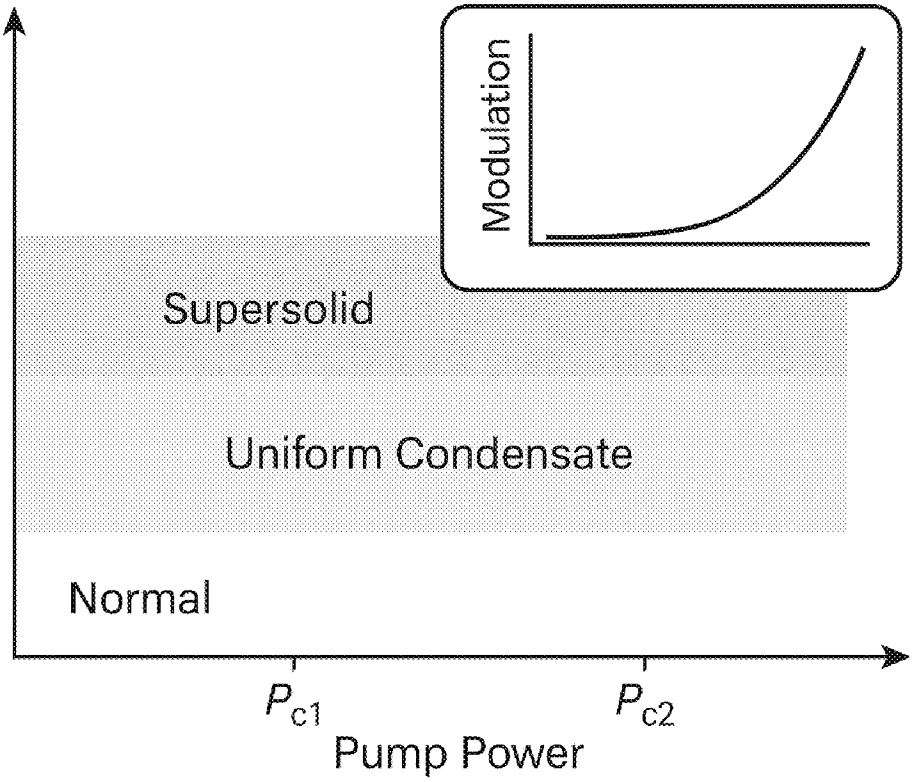

Figure 3. Pump-power phase diagram:

• Below Pc1 – no condensate (normal).

• Pc1 ≤ P < Pc2 – uniform polariton condensate.

• P ≥ Pc2 – χ^3 self-locking drives a supersolid with density modulation depth that grows with pump power (inset).

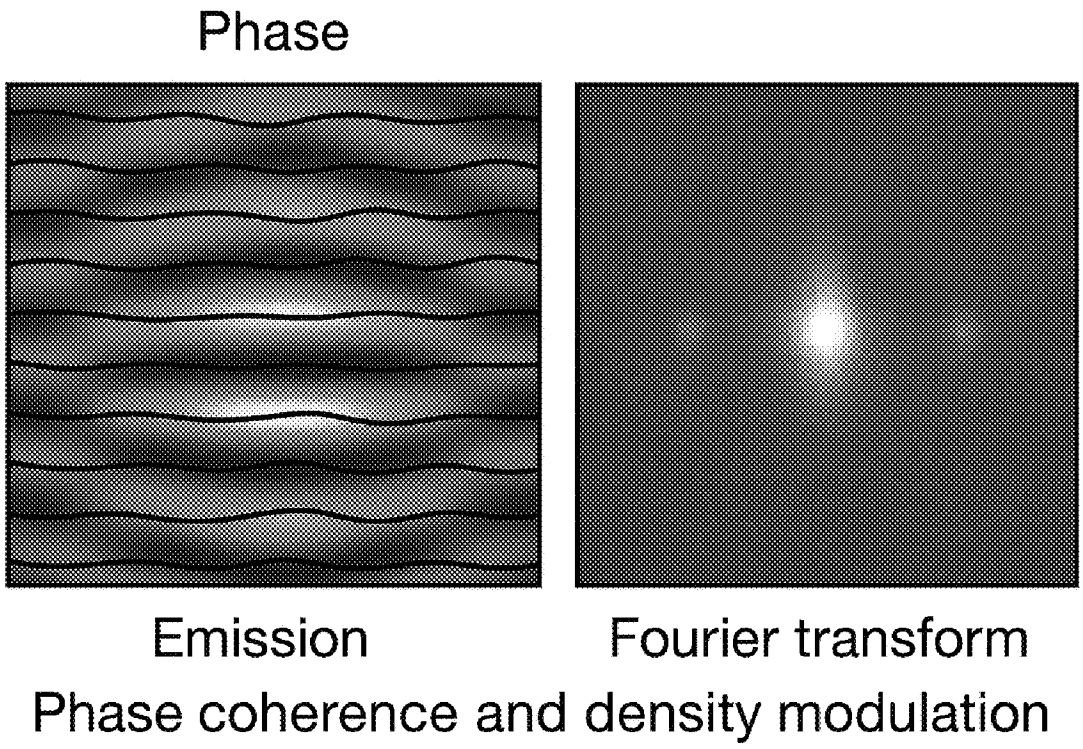

Figure 4. Left: Real-space emission from the supersolid polariton condensate, showing periodic intensity fringes (colour map) overlaid with equal-phase contours (black), evidencing long-range phase coherence.

Right: Fourier transform of the same image reveals the central condensate peak at $k \approx 0$ plus symmetric side-peaks at $\pm k$, confirming the self-organised density lattice.

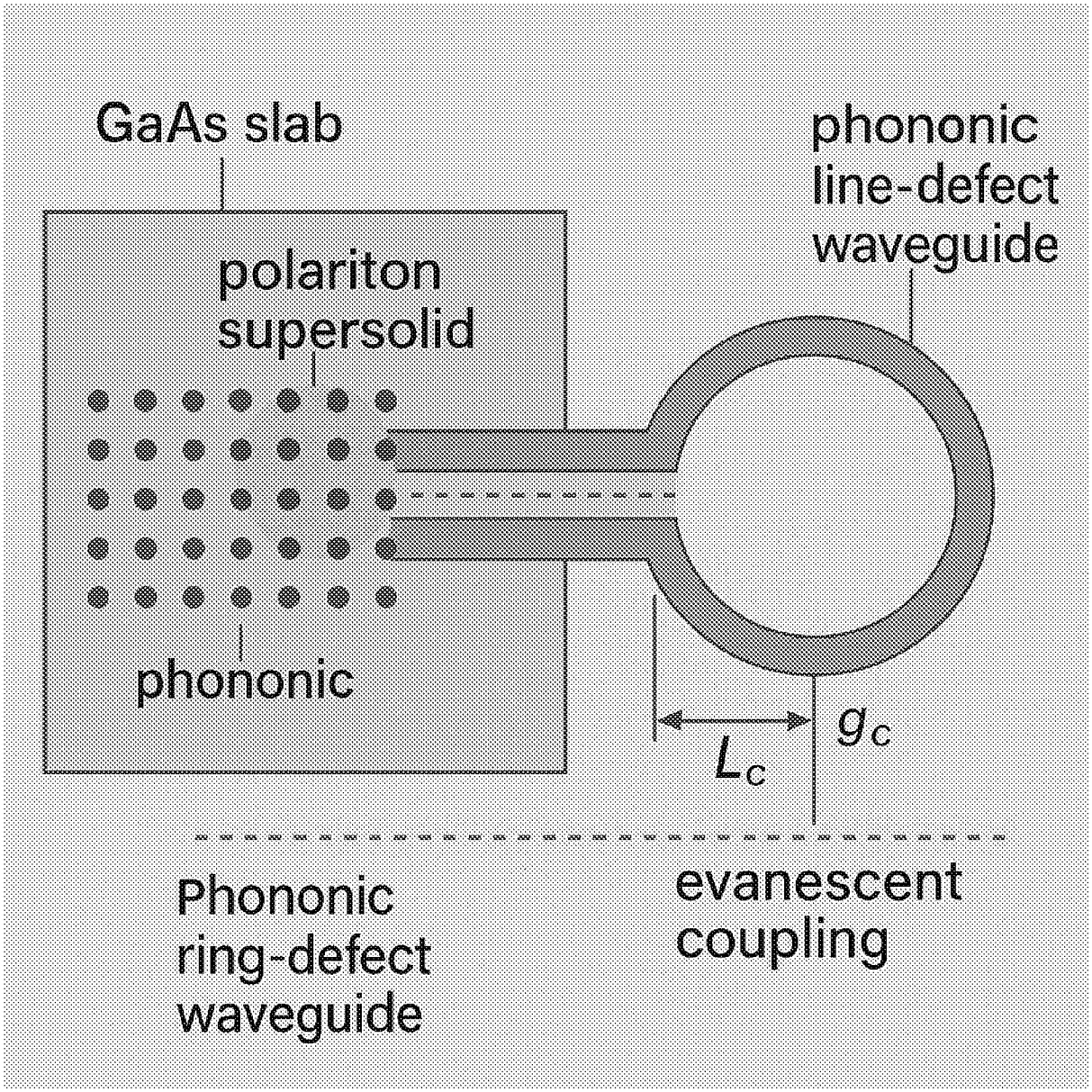

Figure 5. Plan-view layout: the photonic-crystal GaAs slab hosts the polariton supersolid (yellow region). A neighbouring one-row line-defect forms a suspended phononic waveguide that couples (gap gc, length Lc) to a circular phononic ring resonator, enabling extraction and routing of the supersolid's Goldstone-mode vibrations.

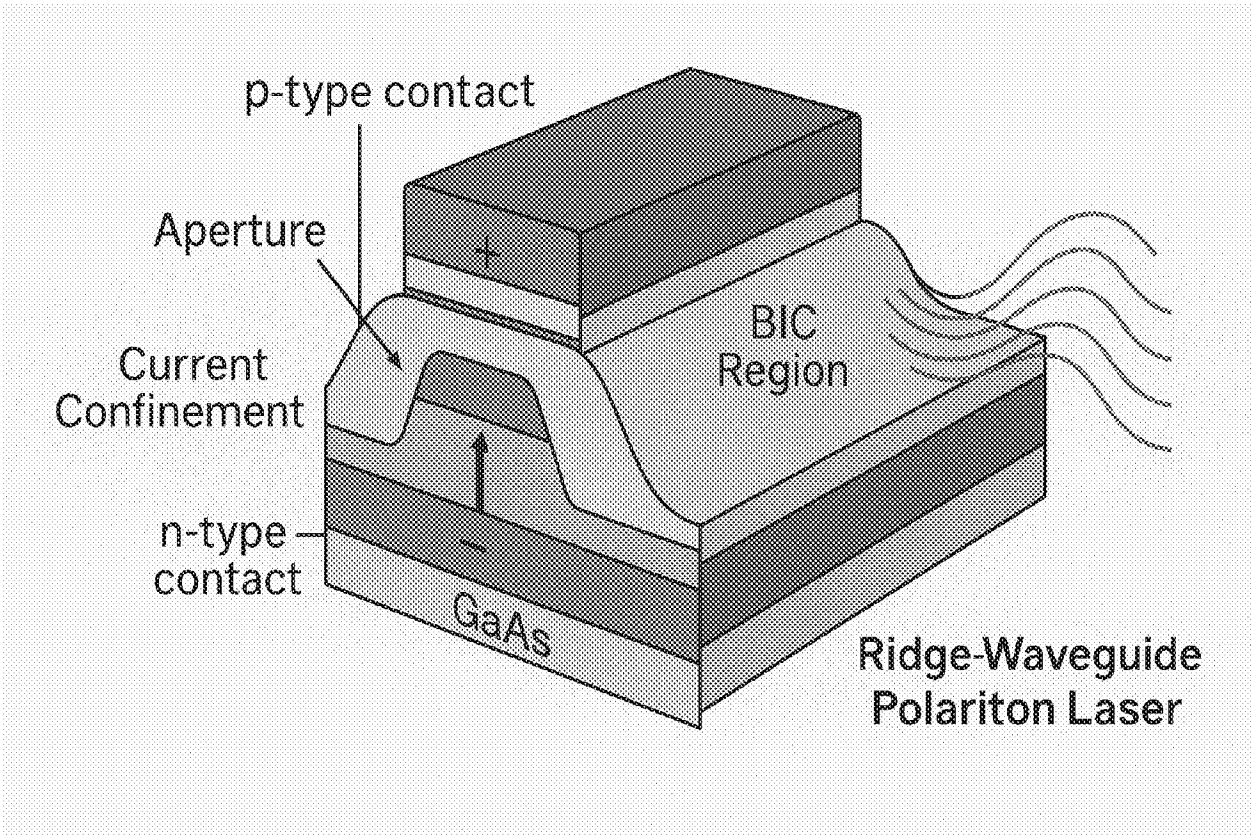

Figure 6. Electrical-injection ridge-waveguide polariton laser variant. Current is confined through an aperture into the BIC region, inducing a supersolid condensate under drive current $I \geq Ic2$. Contacts and confinement layers are labelled.

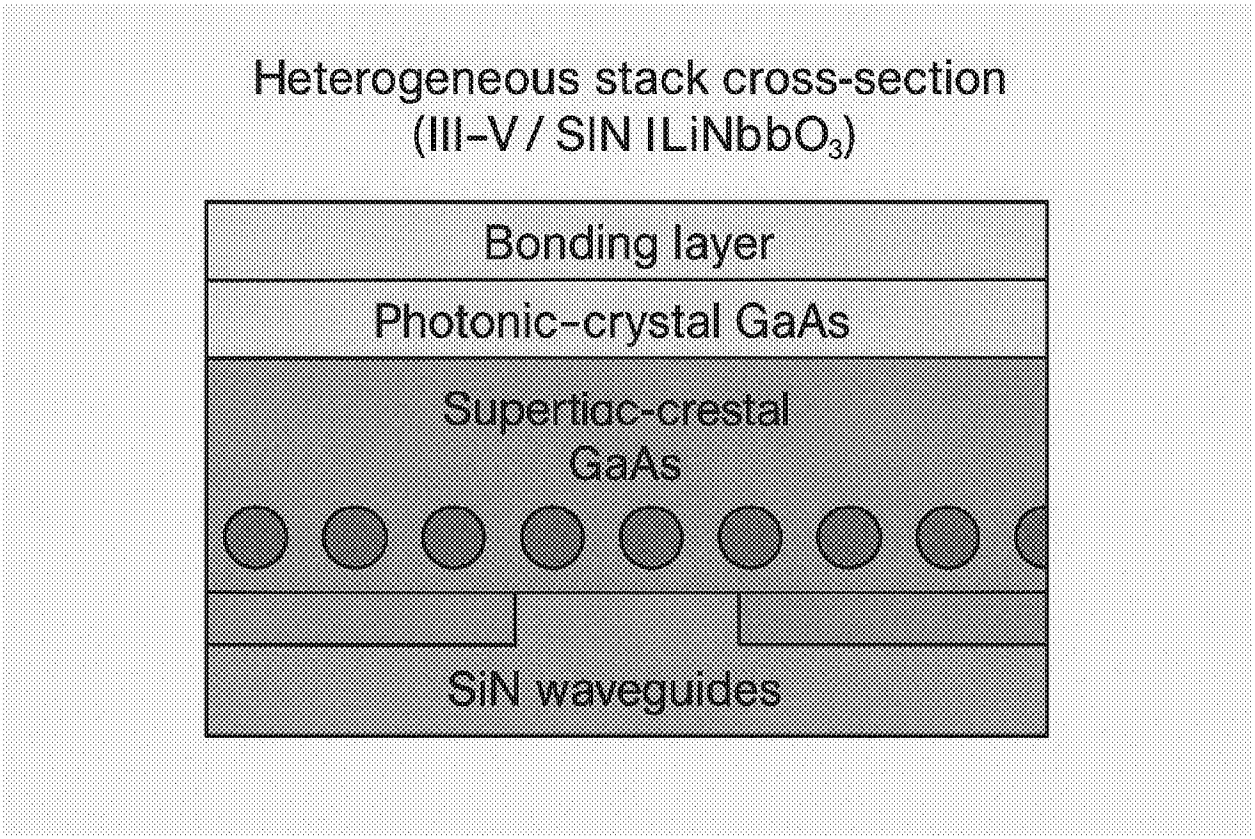

Figure 7. Cross-section of a heterogeneous III–V / SiN / $LiNbO_3$ stack: a bonded thin-film $LiNbO_3$ layer (top) overlies the photonic-crystal GaAs slab that hosts the supersolid polariton lattice (etched holes). Underneath, SiN waveguides route on-chip signals; the bonding layer provides optical and acoustic coupling between tiers.

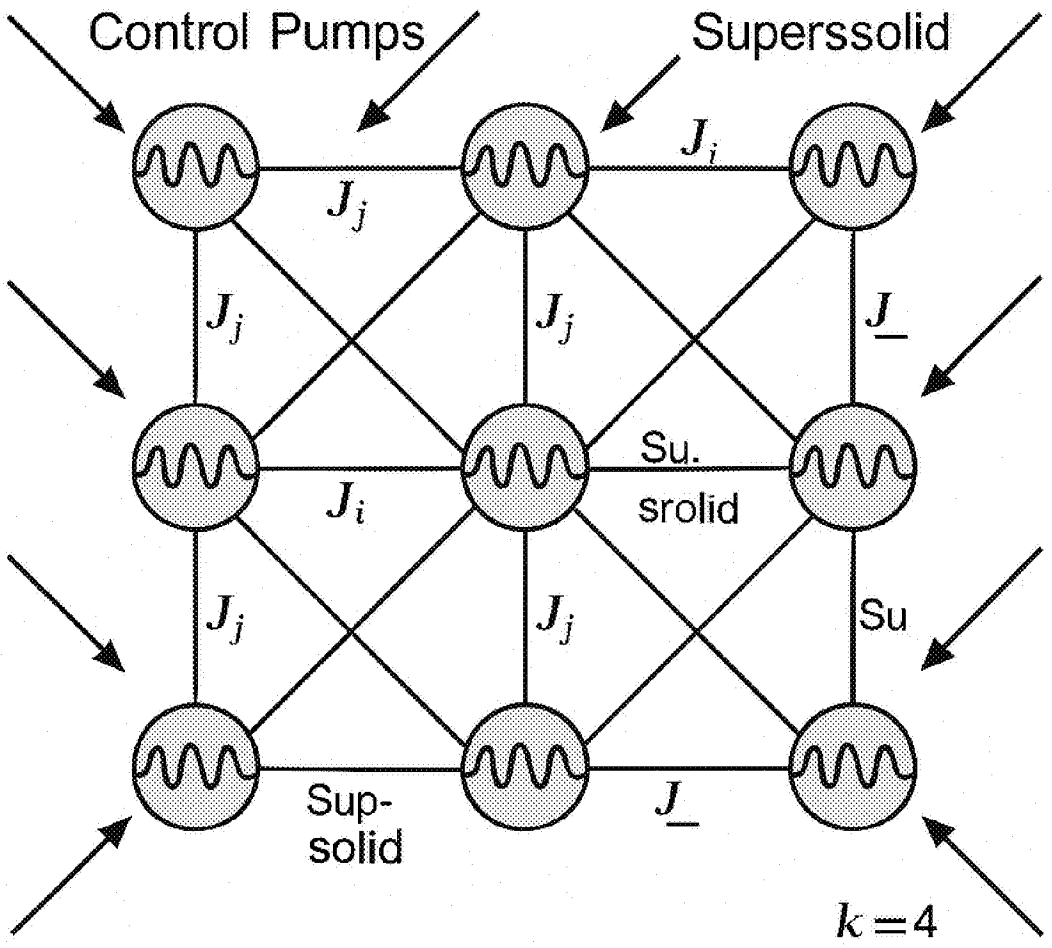

FIG. 8 Array of supersolid cells with couplings and control pumps

Figure 8. Array architecture for quantum simulation: a 4 × 4 grid of polariton supersolid cells (yellow) with programmable nearest-neighbour couplings Jij. Diagonal arrows mark independent pump spots that tune each cell's onsite potential and inter-cell coupling strength, enabling implementation of Ising or Bose–Hubbard Hamiltonians.

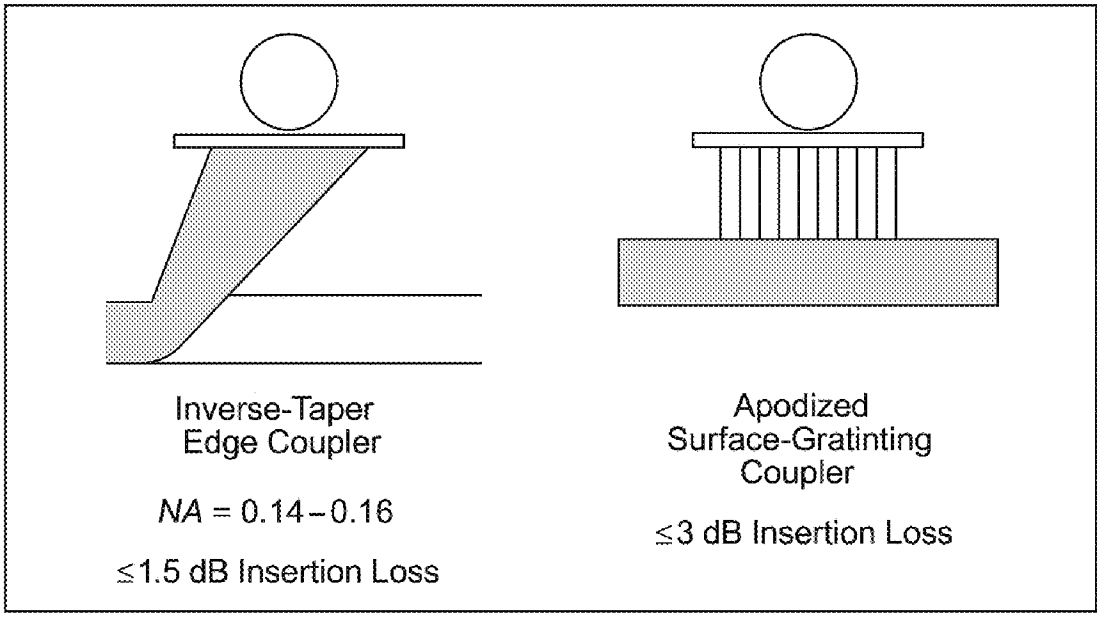

FIG. 9

Edge-Taper and Surface-Grating Fibre-Coupler Geometries

Figure 9. Edge-taper (left) and apodised surface-grating (right) fibre-coupler geometries with key specifications: NA ≈ 0.14–0.16 and ≤ 1.5 dB insertion loss for the inverse-taper edge coupler; ≤ 3 dB insertion loss and ± 2 μm alignment tolerance for the grating coupler.